

## THE INFRARED UNDULATOR PROJECT AT THE VUV-FEL

J. Feldhaus, O. Grimm\*, O. Kozlov, E. Plönjes, J. Rossbach, E. Saldin, E. Schneidmiller, M. Yurkov  
 DESY, Hamburg, Germany

### Abstract

The VUV-FEL at DESY, Hamburg, will be complemented with an undulator producing radiation in the wavelength range (1–200)  $\mu\text{m}$  by autumn 2006. First, it will serve as a powerful radiation source naturally synchronized with the vacuum-ultraviolet (VUV) pulses from the FEL, thus allowing pump-probe experiments with high timing precision. Second, it will help to characterize the longitudinal charge distribution of the short electron bunches in a manner similar to other frequency-domain techniques using infrared radiation currently studied at the VUV-FEL.

### INTRODUCTION

Complementing the VUV-FEL at DESY, Hamburg, with an undulator working in the mid- and far-infrared regime was first proposed in [1]. There is growing interest in using such an undulator delivering up to 10 MW peak power in the THz-regime as a radiation source, allowing especially pump-probe experiments with high temporal resolution using either the infrared or the VUV pulse as probe. In addition, the undulator can be used as a diagnostics tool for longitudinal bunch shape measurements [2]. Funding has now been secured and it is planned to install the undulator described in this paper behind the FEL undulator in late 2006.

A further application under discussion is using the undulator as a radiator for a proposed bunch-length measurement technique based on generating an optical replica of the charge distribution and subsequent analysis with standard frequency-resolved optical gating (FROG) devices [3].

### UNDULATOR DESIGN

The undulator is designed as a planar electromagnetic device. The main parameters are collected in Table 1.

The main electric and cooling parameters allow using infrastructure already existing at DESY. The mechanical design is optimized for the tight spacial situation close to the descending branch of the electron bypass, see Fig. 1.

The undulator magnetic yoke, made from two girders of type 1010 plain carbon steel, supports poles milled to 50  $\mu\text{m}$  precision. The yoke itself rests on a C-shaped support made from non-magnetic steel, limiting a change of the undulator gap due to magnetic forces to no more than 10  $\mu\text{m}$ . The support is equipped with an alignment system

\* Corresponding author. E-Mail: oliver.grimm@desy.de

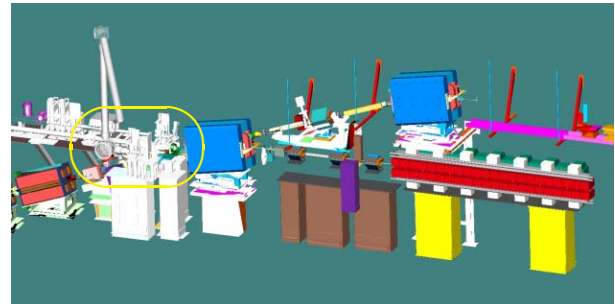


Figure 1: The infrared undulator (on the right, red) as planned to be installed in the VUV-FEL. Radiation out-coupling, focusing, and optionally detection occurs in the encircled region next to the large dipole magnet.

and allows, due to its shape, easy access to the gap, facilitating for example magnetic field measurements.

The windings of the main coils are produced from square pipes of 8.5 mm width, having an aperture of 5.3 mm diameter for circulation of cooling water (the conductor cross-section is thus 50 mm<sup>2</sup>). The electrical isolation is 0.4 mm thick. A basic coil consists of four layers with 15 windings each and a 1 mm diameter copper wire wound around to adjust the field strength. The end poles are wound in a similar manner, though with only one or three layers, and contain separately powered correction windings for adjusting the first and second field integrals.

Using the undulator for the replica-based bunch length diagnostics requires tunability down to wavelengths in the range (0.5–1)  $\mu\text{m}$ , demanding a sufficient field quality at small excitation currents, i.e. good control of remanence effects. This is part of the specification.

### INFRARED BEAM LINE

The infrared radiation will be transported to one of the end stations of the VUV-FEL user facility for pump-probe experiments combining the VUV-FEL with the infrared source. In addition, a laboratory designated for working with the infrared radiation alone is proposed in the user facility. A beam line design into a building next to the dump region of the TTF2 linac is currently kept as fall-back solution in case timely installation of beam line components would otherwise be impossible.

The beam line design into the experimental hall makes use of an existing beam pipe transporting visible synchrotron radiation from the dump magnet, currently used for synchronization purposes. As this pipe has a diam-

Gap	40 mm	Maximum field	1.18 T (K=44 @500 MeV)
Period	40 cm	Total weight	5100 kg
Number of full periods	9	Ampere-turns per coil	27520 A
Number of poles	44	Number of turns	64
Termination pattern	+1/4,-3/4,+1,...,-1,+3/4,-1/4	Maximum current	435 A
Good field region	$\pm 5$ mm ( $\Delta B/B < 3 \times 10^{-3}$ )	Conductor area	50 mm <sup>2</sup>
First field integral	$< 2 \times 10^{-4}$ Tm (@1 T)	Current density	8.7 A/mm <sup>2</sup>
Second field integral	$< 2 \times 10^{-4}$ Tm <sup>2</sup> (@1 T)	Resistance (main coil)	13.1 m $\Omega$
Iron yoke length	4.3 m	Inductance (main coil)	0.11 mH
Total cooling water flow	100l/min	Voltage (main coil)	5.7 V
Water temperature rise	20°C	Total resistance	0.55 $\Omega$
Temperature rise (water cut off)	0.4°C/s	Total inductance	4.4 mH
Total power	104 kW	Total voltage	238 V

Table 1: Main parameters of the infrared undulator.

eter of only 100mm, intermediate focusing elements are needed as shown in Fig. 2 to transport far-infrared radiation efficiently. Plotted in the bottom of that figure are  $2\sigma$  beam radii for this lay-out calculated using Gaussian optics. A restriction towards long wavelengths is the limited aperture of the dump magnet, indicated in blue.

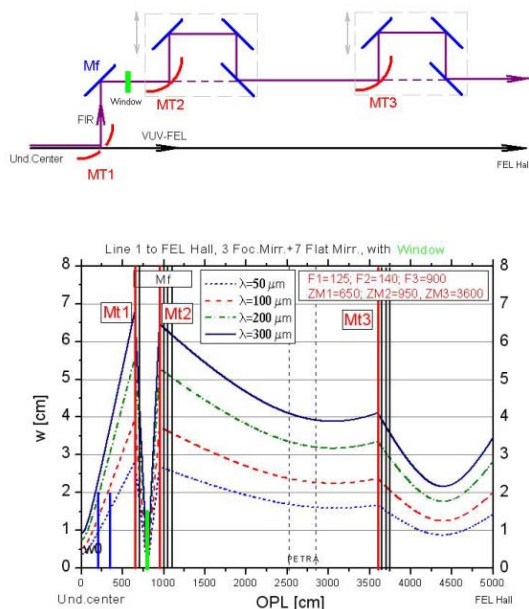


Figure 2: Mirror arrangement (top) and  $2\sigma$  beam radii calculated using Gaussian optics (bottom) for the beam line into the experimental hall.

The accelerator vacuum is separated from the rougher beam line vacuum by a diamond window located at the position of an intermediate focus. A larger crystal Quartz window is foreseen to allow easy viewing and alignment of the out-coupling region. For beam diagnostics, a broadband infrared detector will be installed in the accelerator tunnel, close to the out-coupling port.

Inevitably, the path length for the infrared radiation will

be significantly longer by several meters compared to that of the VUV pulses due to the intermediate focusing stations. To allow nevertheless pump-probe experiments, several options are currently pursued. Conceptually simplest is the combination of radiation from two consecutive bunches (FEL pulse from the second). At 9 MHz repetition rate this corresponds to 33 m path length, thus requiring additional delay of this order on the side of the infrared pulse. Alternatively, a delay line for the VUV-FEL pulses compensating for the path length difference can be fabricated using normal-incidence multilayer mirrors. As such mirrors are only reasonably reflective in a very narrow wavelength band such a design comes at the cost of losing the wavelength tunability of the FEL. Finally, the possibility to accelerate two electron bunches separated by several radio frequency buckets, each giving 23 cm delay at 1.3 GHz, is under investigation.

## RADIATION PROPERTIES

The radiation properties have been calculated numerically using the actual magnetic field of the current undulator design and the paraxial approximation described in [4]. Comparisons with the resonance approximation, as derived, for example, in [5, Chapter 11], show good agreement within the validity of the approximation. In Fig. 3 the normalized transverse intensity distribution of the horizontal polarization component of the fundamental is plotted for two values of K at the position of the out-coupling mirror MT1. The vacuum pipe has a diameter of 35 mm at this position, so part of the radiation cone will be cut due to aperture effects (cf. Fig. 2, bottom).

A typical pulse shape in time-domain for a Gaussian bunch with 1 nC charge and  $\sigma=50\mu\text{m}$  is shown in Fig. 4.

The on-axis spectral distribution of the radiation from a single electron is shown in Fig. 5 at the position of mirror MT1. To get the total spectrum emitted from a bunch this has to be multiplied with the bunch form factor according to (1). The modulus of the form factor for a Gaussian shape and a peaked shaped parametrized in [2] is also shown in the figure.

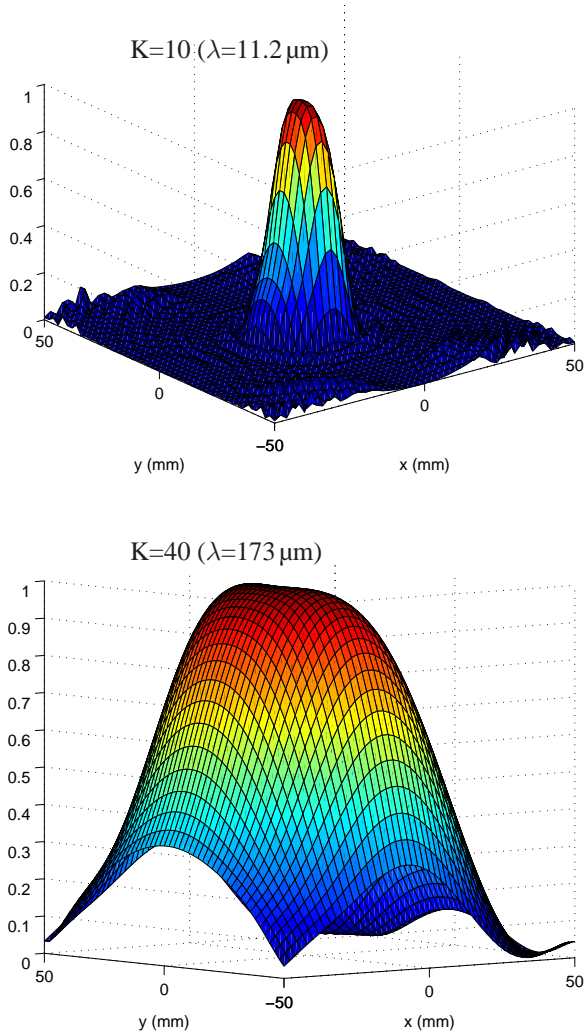


Figure 3: Transverse intensity distribution of the horizontal polarization component (fundamental frequency) at mirror MT1. No aperture effects are considered, normalization to the forward direction.

The resulting total spectrum in forward direction for two values of  $K$  is plotted in Fig. 6. Here, the form factor for the peaked shape has been used. For  $K=10$  the emission spectrum is dominated by small oscillations away from the resonance peak due to the boosting by the form factor. In case the actual bunch shape has structures on a smaller scale, the form factor will have non-negligible values up to higher frequencies, cf. (2), and the resonance peak can become more pronounced.

Diffraction at beam pipe and mirror apertures will be considered in currently on-going calculations using a Fourier optics approach. These will yield the full transmission characteristic of the beam line.

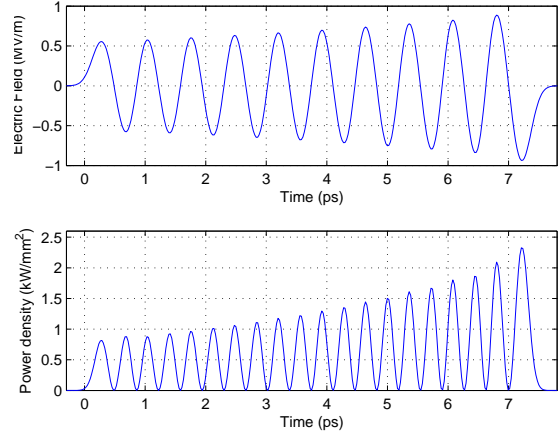


Figure 4: Electric field and power density in time-domain at position of mirror MT1 on-axis for a 1 nC Gaussian bunch with  $\sigma=50 \mu\text{m}$ . Edge effects not taken into account.

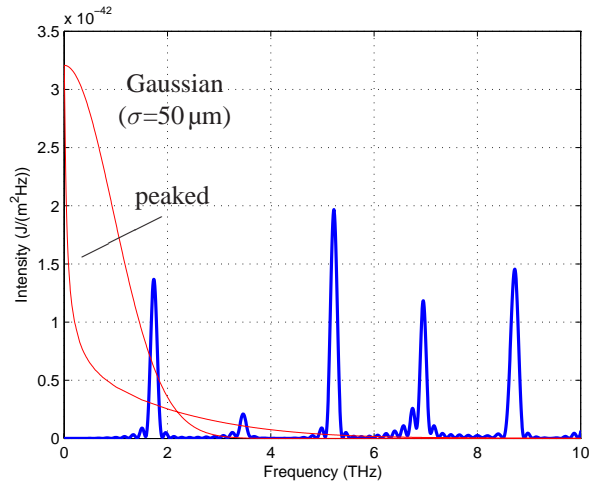


Figure 5: Single electron spectrum on-axis for  $K=40$ . The form factors for a Gaussian bunch and for a typical peaked bunch shape in the VUV-FEL given in [2] are also shown.

## LONGITUDINAL BEAM DIAGNOSTICS

Similar to synchrotron or transition radiation, the bunch shape is imprinted on the undulator radiation spectrum  $dU/d\lambda$  through the form factor  $F(\lambda)$ ,

$$\frac{dU}{d\lambda} = \left( \frac{dU}{d\lambda} \right)_0 \left( N + N(N-1) |F(\lambda)|^2 \right), \quad (1)$$

where  $(dU/d\lambda)_0$  is the emission spectrum of one single electron,  $N$  is the total number of electrons, and the form factor is the Fourier transform of the normalized longitudinal charge distribution  $S(z)$  ( $\int_{-\infty}^{\infty} S(z) dz = 1$ ),

$$F(\lambda) = \int_{-\infty}^{\infty} S(z) \exp\left(\frac{-2\pi i}{\lambda} z\right) dz. \quad (2)$$

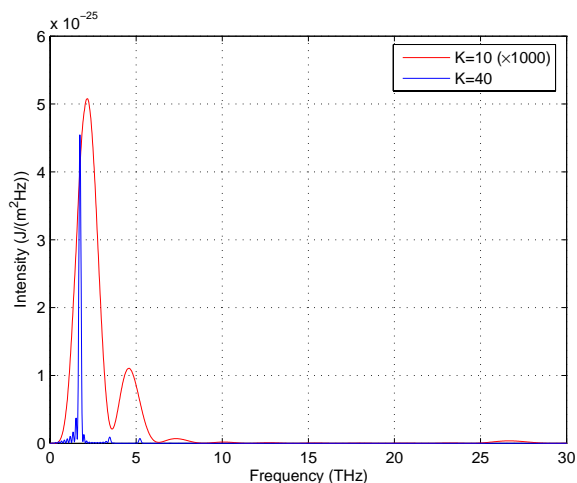


Figure 6: Total spectrum on-axis at position of mirror MT1 for a 1 nC bunch using a shape as parametrized in [2] for K values of 10 (curve multiplied by 1000) and of 40.

The basic assumption in the derivation of these equations is that each electron generates a time-dependent electric field at a given position that is the same for all electrons except a time delay (corresponding to a spacial distance).

Measurement of the total spectrum and knowledge of the number of electrons and the single-electron spectrum then gives access to the modulus of the form factor. The final step of inverse Fourier transforming this to arrive at the bunch shape requires knowledge of the phase of the Fourier transform. This, although not directly measured, is partially determined by the modulus through a Kramers-Kronig relation [6]. If one writes for the complex form factor  $F(\omega) = |F(\omega)| \exp(i\psi(\omega))$ , with  $\omega$  the angular frequency, then

$$\psi(\omega) = -\frac{2\omega}{\pi} \int_0^{\infty} \frac{\ln(|F(x)|/|F(\omega)|)}{x^2 - \omega^2} dx$$

yields a phase consistent with the measured modulus (but the solution is not unique) [7].

The electromagnetic undulator effectively replaces the spectrometer used in other frequency-domain approaches by its tuning capability, thus avoiding frequency-resolved measurements in (1). A pre-requisite for this to work is that the major intensity contribution is from the resonance peak. Also, good knowledge of the beam line transmission characteristics and the detector response is necessary.

The possibility to tune the undulator down to 1  $\mu\text{m}$  will give the unique chance to detect structures of the bunch on this scale, even if the precise longitudinal shape cannot be determined. Such micro-bunching is currently not excluded and could have a significant effect on beam dynamics in bunch compressors.

## REFERENCES

- [1] B. Faatz et al., Nucl. Instr. Meth. **A475**, 363 (2001)
- [2] G. Geloni et al., DESY 03-031 (March 2003)
- [3] E.L. Saldin et al., DESY 04-126 (July 2004)
- [4] G. Geloni et al., DESY 05-032 (February 2005)
- [5] H. Wiedemann, *Particle Accelerator Physics II*, Springer (1995)
- [6] J.S. Toll, Phys. Rev. **104**, 1760 (1956)
- [7] R. Lai, A.J. Sievers, Nucl. Instr. Meth. **A397**, 221 (1997)